Class. Quantum Grav. **25** (2008) 184003 (8pp) doi:10.1088/0264-9381/25/18/184003

Noise studies during the first Virgo science run and after

F Acernese[1,2], M Alshourbagy[3,4], P Amico[5,6], F Antonucci[7], S Aoudia[8], K G Arun[9], P Astone[7], S Avino[1,10], L Baggio[11], G Ballardin[12], F Barone[1,2], L Barsotti[3,4], M Barsuglia[9], Th S Bauer[13], S Bigotta[3,4], S Birindelli[3,4], M A Bizouard[9], C Boccara[14], F Bondu[8], L Bosi[5], S Braccini[3], C Bradaschia[3], A Brillet[8], V Brisson[9], D Buskulic[11], G Cagnoli[15], E Calloni[1,10], E Campagna[15,16], F Carbognani[12], F Cavalier[9], R Cavalieri[12], G Cella[3], E Cesarini[15,17], E Chassande-Mottin[8], S Chatterji[7], F Cleva[8], E Coccia[18,19], C Corda[3,4], A Corsi[7], F Cottone[5,6], J-P Coulon[8], E Cuoco[12], S D'Antonio[18], A Dari[5,6], V Dattilo[12], M Davier[9], R De Rosa[1,10], M Del Prete[3,20], L Di Fiore[1], A Di Lieto[3,4], M Di Paolo Emilio[18,21], A Di Virgilio[3], V Fafone[18,19], I Ferrante[3,4], F Fidecaro[3,4], I Fiori[12], R Flaminio[22], J-D Fournier[8], S Frasca[7,23], F Frasconi[3], L Gammaitoni[5,6], F Garufi[1,10], E Genin[12], A Gennai[3], A Giazotto[3,12], V Granata[11], C Greverie[8], D Grosjean[11], G Guidi[15,16], S Hamdani[12], S Hebri[12], H Heitmann[8], P Hello[9], D Huet[12], P La Penna[12], M Laval[8], N Leroy[9], N Letendre[11], B Lopez[12], M Lorenzini[15,17], V Loriette[14], G Losurdo[15], J-M Mackowski[22], E Majorana[7], N Man[8], M Mantovani[12], F Marchesoni[5,6], F Marion[11], J Marque[12], F Martelli[15,16], A Masserot[11], F Menzinger[12], C Michel[22], L Milano[1,10], Y Minenkov[18], S Mitra[8], J Moreau[14], N Morgado[22], S Mosca[1,10], B Mours[11], I Neri[5,6], F Nocera[12], G Pagliaroli[18], C Palomba[7], F Paoletti[12,3], S Pardi[1,10], A Pasqualetti[12], R Passaquieti[3,4], D Passuello[3], F Piergiovanni[15,16], L Pinard[22], R Poggiani[3,4], M Punturo[5], P Puppo[7], O Rabaste[8], P Rapagnani[7,23], T Regimbau[8], F Ricci[7,23], I Ricciardi[1,10], A Rocchi[18], L Rolland[11], R Romano[1,2], P Ruggi[12], D Sentenac[12], S Solimeno[1,10], B L Swinkels[12], R Terenzi[18], A Toncelli[3,4], M Tonelli[3,4], E Tournefier[1,11], F Travasso[5,6], G Vajente[4,24], J F J van den Brand[13,25], S van der Putten[13], D Verkindt[11], F Vetrano[15,16], A Viceré[15,16], J-Y Vinet[8], H Vocca[5] and M Yvert[11]

[1] INFN, Sezione di Napoli, Italy
[2] Università di Salerno, Fisciano (SA), Italy
[3] INFN, Sezione di Pisa, Italy
[4] Università di Pisa, Pisa, Italy
[5] INFN, Sezione di Perugia, Italy
[6] Università di Perugia, Perugia, Italy
[7] INFN, Sezione di Roma, Italy
[8] Lab. Artemis, Univ. NSA, Obs. Côte d'Azur, CNRS, BP 4229 06304 Nice, Cedex 4, France
[9] LAL, Univ. Paris-Sud, IN2P3/CNRS, Orsay, France
[10] Università di Napoli 'Federico II' Complesso Universitario di Monte S. Angelo, Italy
[11] Laboratoire d'Annecy-le-Vieux de Physique des Particules (LAPP), IN2P3/CNRS, Université de Savoie, Annecy-le-Vieux, France
[12] European Gravitational Observatory (EGO), Cascina (PI), Italy

0264-9381/08/184003+08$30.00

[13] National Institute for Subatomic Physics, NL-1009 DB Amsterdam, The Netherlands
[14] ESPCI, Paris, France
[15] INFN, Sezione di Firenze, Sesto Fiorentino, Italy
[16] Università degli Studi di Urbino 'Carlo Bo', Urbino, Italy
[17] Università degli Studi di Firenze, Firenze, Italy
[18] INFN, Sezione di Roma Tor Vergata, Roma, Italy
[19] Università di Roma Tor Vergata, Roma, Italy
[20] Università di Siena, Siena, Italy
[21] Università dell'Aquila, L'Aquila, Italy
[22] LMA, Villeurbanne, Lyon, France
[23] Università 'La Sapienza', Roma, Italy
[24] Scuola Normale Superiore, Pisa, Italy
[25] Vrije Universiteit, NL-1081 HV Amsterdam, The Netherlands

E-mail: irene.fiori@ego-gw.it

Received 4 April 2008, in final form 30 June 2008
Published 2 September 2008
Online at stacks.iop.org/CQG/25/184003

Abstract
The first Virgo long science run (VSR1) lasted 136 days, from 18th May 2007. During the run several noise sources were identified and reduced; this significantly improved the detector sensitivity between the start and the end of the run. We describe three noise studies, showing how data monitoring programs and simple analysis tools permitted the first detection of the noise and provided useful information regarding its origin.

PACS numbers: 04.80.Nn, 95.55.Ym, 43.50.Rq, 05.40.Ca

(Some figures in this article are in colour only in the electronic version)

1. Introduction

Virgo is a power-recycled Michelson interferometer (ITF) with 3 km long Fabry–Perot cavities in its arms, aimed to detect gravitational wave signals in the 10 Hz to 10 kHz frequency band [1]. The detector is in the final commissioning phase, and the search for control and environmental noise sources is a major activity. The VSR1 run took place between 18th May and 1st October 2007, the detector was locked in a science mode for 81% of the time [2]. Investigations were performed during the run to identify the noise sources limiting the ITF sensitivity. The mitigation of some noise sources contributed to increasing the NS–NS horizon distance [2] from 3.5 Mpc at the beginning to 4.5 Mpc at the end of the run.

In this paper we illustrate three noise studies conducted during VSR1 and right after. These are: (i) the noise produced by some piezo-electric actuators (section 2), (ii) the seismic and acoustic noise produced by air conditioning devices (section 3) and (iii) the identification of the internal modes of the suspended mirrors (section 4). We describe the role played in the noise search by simple data analysis tools and monitoring programs such as the online computation of band limited RMS of noise, the identification of spectral lines, the time–frequency monitor of ITF signals and the in-time analysis of transient events. The investigated noises as well the analysis tools are common to other gravitational-wave (GW) experiments and to the GW scientific community who might be interested in listening to our experience.

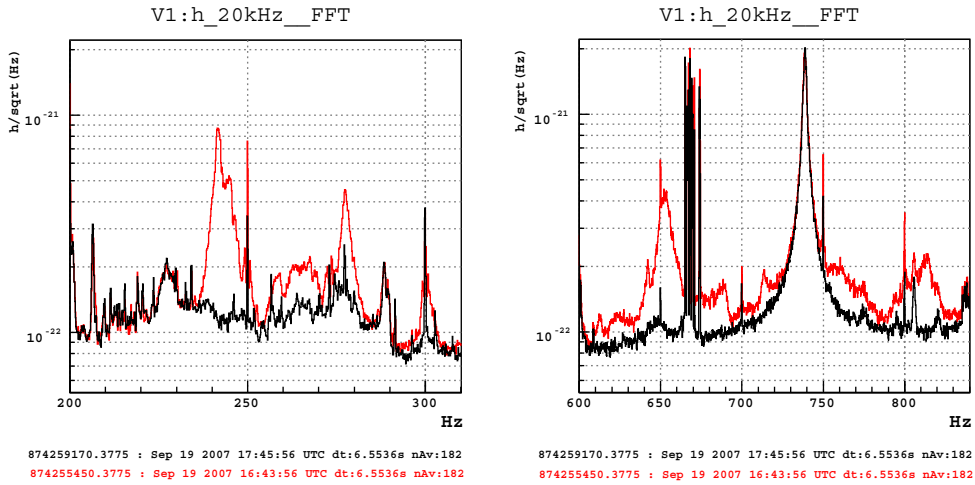

Figure 1. Virgo sensitivity during VSR1 in the two frequency regions of the mystery noise peaks, before (red curves) and after (black) the removal of the noise.

(This figure is in colour only in the electronic version)

In this paper we focus on the description of the methods adopted in the noise search, possibly avoiding details that are peculiar to the Virgo design. Much of the described noise searches are based on unproven theories and a provisional working hypothesis, as it is typical for the detectors commissioning work.

2. Noise from PZT actuators on the suspended injection bench

Since the start of VSR1, a noise was present in the dark fringe signal which consisted of correlated non-stationary structures in the frequency region between 100 Hz and 1 kHz, the most intense structures peaked at 243 Hz and 652 Hz (figure 1). We named it the *mystery noise*.

This noise originated from two piezo-electric actuators (PZT) placed on the suspended input bench (SIB) which carries the two input mirrors of the triangular input mode cleaner (IMC) optical cavity. These two mirrors are assembled in one structure we name the *dihedron*. The two PZT are powered with a constant voltage and used to keep in position the mirrors which align the beam into the reference optical cavity, also located on the SIB. The residual high frequency noise of the supplied voltage was shaking the PZT supports and the bench itself[26]. The SIB movement then produced beam jitter and length noise in the IMC, which polluted the sensitivity.

As was clear *a posteriori*, revealing the mystery noise was made difficult by the fact that another non-stationary uncorrelated noise of a similar amplitude partially overlapped with the mystery noise frequencies (see section 3). The VSR1 long observation time permitted us to correlate the slow fluctuation of the mystery noise with other noise structures in the dark fringe signal and in other signals. These studies were performed with simple online analysis programs. We briefly illustrate these studies, which were conducted to finally locate and remove the noise source toward the end of VSR1.

[26] We suspect that the frequency of the mystery noise peaks, 240 Hz and 650 Hz, correspond to mechanical resonances of the PZT supports. We measured the mechanical modes of supports of similar size and found values in the 200–700 Hz range.

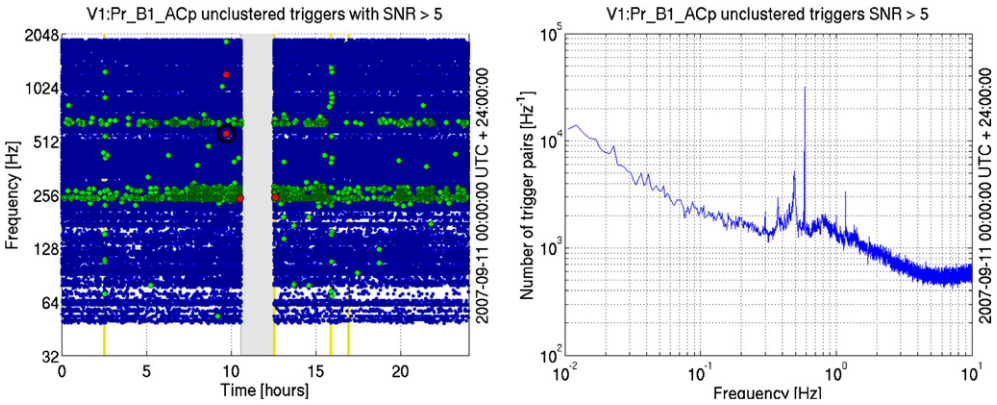

Figure 2. Left: *QOnline* plot showing the time–frequency distribution of transient events clustering at the mystery noise frequencies. Each event detected with SNR > 5 is represented with a green dot at the event center frequency and time. Right: spectrum of pairwise time delay between events.

(1) During the run we monitored the dark fringe RMS noise in the mystery noise frequency bands, using the *NonStatMoni* online tool [8]. The spectral analysis of the RMS signal permits us to detect the peculiar frequencies which modulate the noise amplitude. We identified periods during which the noise was deeply modulated at a frequency (42 mHz) corresponding to a resonant mode, the super-attenuator [11], which suspends the input optical bench (SIB) of the input mode cleaner (IMC) cavity.

(2) The *QOnline* program monitors the dark fringe signal for transient events. It provides information on the time and frequency of the events and on the event rate [6]. The *QOnline* detected, in correspondence to periods when the mystery noise was particularly intense, the occurrence of bursts of transient events clustered at the mystery noise frequencies. Figure 2 (left) shows one of these periods. The rate of the transient events peaks at 372 mHz and 490 mHz (figure 2 (right)). These frequencies correspond to the low frequency mechanical modes of the SIB suspension as well.

(3) The *SpectroMoni* program [9] computes and displays in-time spectrograms of several ITF channels. This tool permits an easy visual inspection and correlation of very slow noise non-stationarities (time scales longer than 10 min). Inspecting the spectrograms we identified a few periods, lasting up to a few days (one example in figure 3), during which the most intense mystery noise structures had amplitude fluctuations common to other structures which, according to a finite element model simulation [10], would be resonant modes of the dihedron.

(4) We measured the mechanical resonances of the suspended injection bench including the dihedron. We shaked the SIB while the IMC was locked in a standalone mode. High-Q modes were found to reasonably match the predicted dihedron modes (83, 159 and 173 Hz). Additionally, low-Q modes were found in correspondence with some of the mystery noise frequencies (278, 652 and 813 Hz).

These studies provided evidence that the mystery noise was modulated by alignment fluctuations of the suspended input bench (items 1 and 2)[27]. The modulation frequencies

[27] This information, however, was not sufficient to locate the mystery noise source in the IMC since, at the noise frequencies, the IMC length is locked to the common mode of the ITF arms [3] and it cannot be disentangled from the frequency noise originating in the rest of the ITF.

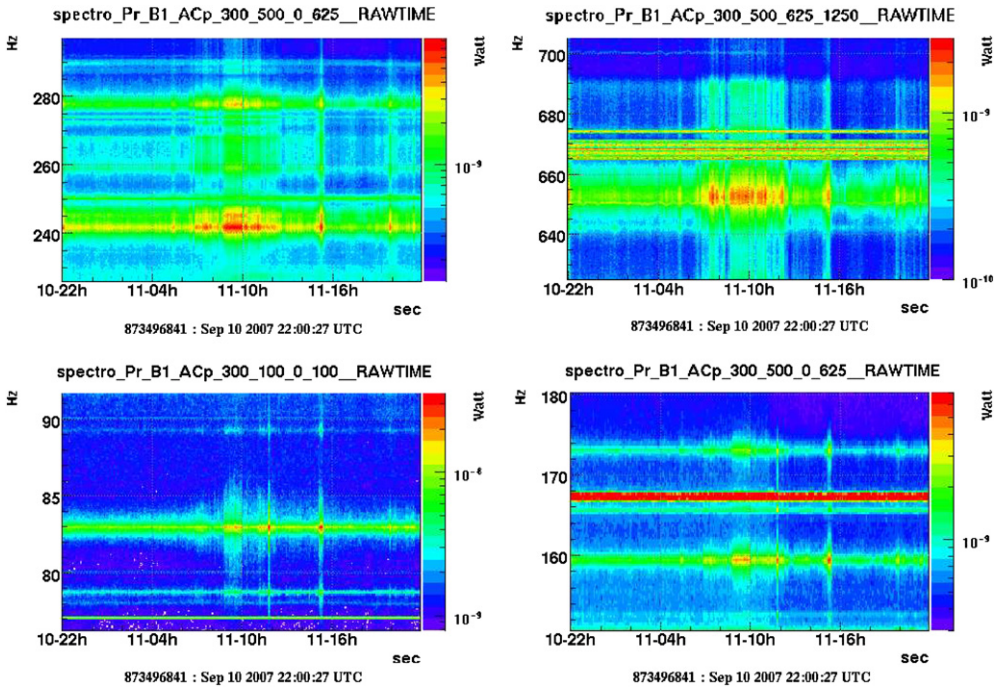

Figure 3. Spectrograms of the dark fringe photodiode signal. The plots show, over a 24 h period, the common amplitude fluctuation of the mystery noise peaks (two upper plots) and of other peaks (83, 159 and 173 Hz) found then to be resonances of the IMC dihedron (two bottom plots).

corresponded to some mechanical modes of the SIB super-attenuator suspension and of the SIB itself (items 3 and 4). These observations (mainly 3 and 4) lead us to the hypothesis that the mystery noise originated from a device located on the SIB which vibrates and shakes the bench (and the dihedron)[28].

The noise was in fact due to PTZ drivers on the SIB. A second-order low-pass filter at 0.1 Hz was added to the dc voltage driving the PZTs. Figure 1 shows the ITF sensitivity improvement consequent to this intervention. The NS–NS horizon distance increased by 0.5 Mpc, and the stationarity (peak-to-peak fluctuation of RMS noise) of the dark fringe signal in the ranges 200–300 Hz and 600–900 Hz improved by at least a factor of 4. The number of transient events detected by *QOnline* drastically decreased.

3. Noise from the air conditioning devices

At the end of VSR1 many of the structures limiting the Virgo sensitivity up to few hundred Hz were due to the noise from back-scattered light and input beam jitter. This noise was sustained by seismic and acoustic environmental disturbances produced mainly from the air conditioning devices (HVAC). The first prompt indication was provided by an occasional cutoff of the mains power which occurred during VSR1 and which caused the shut down of

[28] We evaluated two alternative noises which could shake the bench at frequencies above 100 Hz: (i) a residual seismic noise transmitted by the SIB suspension and (ii) the noise current in the coils acting on the SIB for the slow IMC alignment control. For both the projected noise was more than two orders of magnitude smaller than the mystery noise.

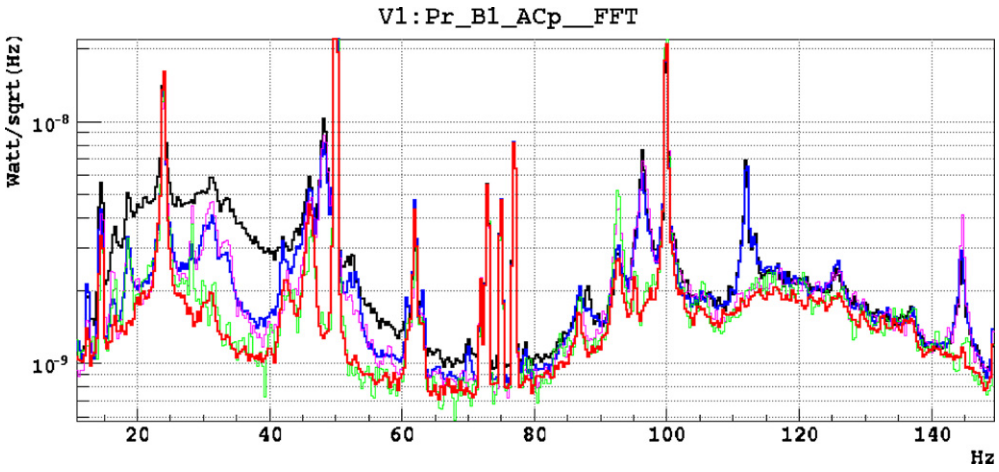

Figure 4. Noise reduction in the dark fringe photodiode signal due to the progressive switchoff of air conditioning devices: the air fans of the north-end experimental hall (blue line), the air fans of the central experimental hall (magenta line), the water pump of the central hall HVAC (green line) and the air fans of the clean rooms HVAC (red line).

(This figure is in colour only in the electronic version)

all the air conditioning devices and a sudden rise of the horizon distance from 4.2 Mpc to 4.8 Mpc.

During VSR1 we monitored the coherence between the dark fringe and seismic and acoustic probes to provide evidence of environmental noise directly coupling to the ITF [4], but we found no significant coherence[29]. The switchoff of the air conditioning units was the only prompt way this noise could be pinned down.

Switch-off tests conducted right after VSR1 permitted us to characterize the noise contribution of each single HVAC device [12]. Figure 4 shows the dark fringe noise reduction associated with the switchoff of the air fan of the north-end experimental hall and of the HVAC devices inside the central building. Understanding the noise coupling paths is important, as well as reducing the seismic and acoustic emissions from the machines, and we worked on these two aspects.

We suspected that the dominant coupling of the environmental acoustic and seismic noise to the dark fringe occurred through parasitic light beams which hit seismically excited surfaces, are phase modulated by the vibration, and then are scattered back into the main beam path.

At the north-end experimental hall the back-scattering processes might occur at the level of the optical components on the external bench which are used to guide and read out the light transmitted by the ITF arm. The noise associated with the HVAC of the north-end experimental hall did in fact reduce consequently to some mitigation actions we performed on the optical bench. These actions consisted mainly of: (i) a better damping of parasitic beams and (ii) the replacing of some beam dumps which, in laboratory measurements, were found to scatter a significant fraction of the impinging light[30].

[29] The lack of coherence indicates a non-linear coupling between the dark fringe and the seismic noise, which is the case for the phase noise from back-scattered light processes [5].

[30] We characterized several commercial and custom optical components by measuring the light scattered at the 45° angle with respect to an incoming laser beam. Some components were scattering up to 10^4 ppm of the incoming light.

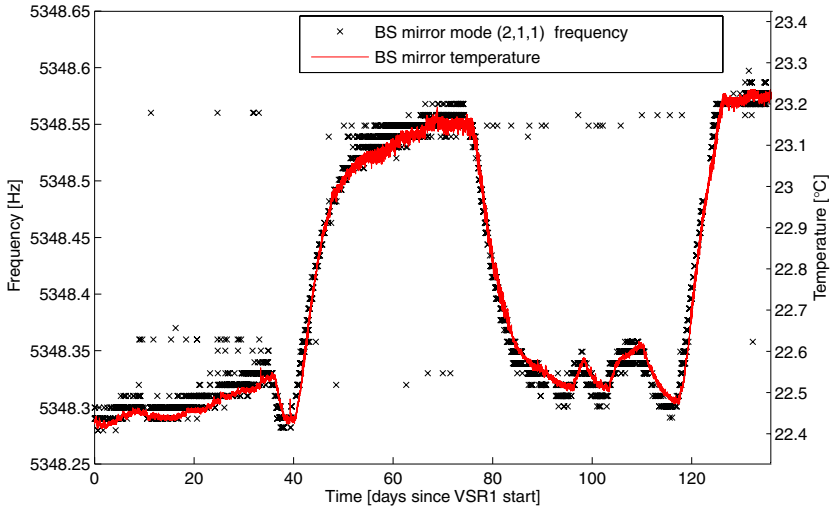

Figure 5. The frequency evolution during VSR1 of the (2, 1, 1) 'butterfly' mode of the beam-splitter (BS) mirror (black markers) matches the evolution of the temperature of the vacuum tower housing the mirror and its suspension (red line). The order of the mode is determined by comparing the average frequency to the prediction of a finite-element model of the mirrors [14].

(This figure is in colour only in the electronic version)

The environmental noise in the central experimental hall was found to couple at the detection port. In particular, diffused light processes occur at the output Brewster window[31] and at the vacuum tank housing the suspended detection bench (SDB). This was shown in various ways: for example by measuring coherence between the dark fringe noise and seismic probes monitoring the vacuum tank wall at these locations, and also by observing that the dark fringe noise was very sensitive to the mechanical excitations or slight mechanical modifications of these parts. The plan is to replace the output Brewster window with one cryogenic vacuum tube to preserve the high vacuum by trapping particles passing through the link.

For this summer, we have planned a shutdown of some works to reduce the acoustic and seismic noise emissions of HVAC devices in the ITF environment. These comprise: (i) the reduction of the air flux in the inlet and outlet ducts, (ii) the insertion of soft joints to decouple the air ducts to the machine vibrations and (iii) the installation of damping pads to reduce vibrations transmitted through the floor.

4. Identification of mirror modes

The internal resonances of the suspended mirrors, thermally excited, produce frequency peaks (lines) in the sensitivity curve. The *LineMonitor* online program extracts the information on the frequency peaks from the dark fringe signal[32]. For each identified peak the value of its central frequency, spectral amplitude and SNR is stored in one *MySQL* database table. A web

[31] In order to preserve the ITF high vacuum, the vacuum volume housing the suspended output bench is isolated by a glass plate placed at the Brewster angle with respect to the output beam.

[32] The algorithm used [7, 8] first estimates the signal spectral background and then searches the spectrum for local maxima whose amplitude is at least four times above the background (SNR $>$ 4). The dark fringe signal is examined at time steps of 300 s and with a spectral resolution of 0.01 Hz.

interface [13] permits easy and fast access to the data, display of time–frequency information and matching to a list of known lines. This tool permits quick browsing through the VSR1 full dataset (4.5 months long) to look for appearing/disappearing lines, or drifts of lines frequency, which can then easily be correlated with other ITF control signals or environmental probes.

The *LineMonitor* data collected during VSR1 were used to identify several internal modes of the Virgo suspended mirrors. The frequency peaks are assigned to mirrors by correlating their slow drift during VSR1 with the variation of the environmental temperatures measured close to the vacuum tower housing the mirror suspension. Figure 5 shows one example. We identified in total 16 modes, whose average frequency is between 4 kHz and 12 kHz, of our six suspended large mirrors.

5. Conclusions

We have illustrated three studies of the Virgo noise conducted during the first long science run and right after. These studies permitted us to characterize some noise sources limiting the detector sensitivity. In one case the identified source of the noise was removed before the end of the run, significantly improving the sensitivity. We described the techniques adopted in the noise investigation, and the use made of simple data analysis tools and monitor programs. The RMS monitor, the spectrogram monitor and the monitor of transient events helped to correlate the noise in different channels and to identify the typical modulation frequencies of the noise non-stationarity. Then experimental tests allowed us to locate the source of this noise and to remove it.

The monitor of spectral lines proved useful to identify noise sources by correlating the frequency evolution of lines to other auxiliary channels. We show how we identified several structural modes of the mirrors by correlating them to the environmental temperature close to the mirrors. Our experience with the environmental noise produced by the air conditioning devices, as well as the noise produced by the piezo-electric actuators on the suspended optical bench, might give useful indications for the study and design of other present and future GW detectors.

References

[1] Virgo Collaboration 1997 *Final Design Report* VIR-TRE-DIR-1000-13
[2] Acernese F *et al* 2008 Virgo status *Class. Quantum Grav.* **25** 184001
[3] Barsotti L 2007 The control of the Virgo interferometer for gravitational waves detection *PhD Thesis* University of Pisa
[4] Acernese F *et al* 2007 Analysis of noise lines in the Virgo C7 data *Class. Quantum Grav.* **24** S433–43
[5] Smith M R 1998 *Up-Conversion of Scattered Light Phase Noise from Large Amplitude Motion* LIGO-T980101-00-D
[6] The *QOnline* monitor of burst events http://wwwcascina.virgo.infn.it/MonitoringWeb/Bursts
[7] Virgo Collaboration 2005 A simple line detection algorithm applied to Virgo data *Class. Quantum Grav.* **22** S1189–96
[8] Vajente G 2008 NonStatMoni Technical Description VIR-004A-08
[9] Virgo monitoring spectrograms http://wwwcascina.virgo.infn.it/MonitoringWeb/Spectro
[10] Puppo P 2006 *Measurements of the Modes of the Dihedron* VIR-NOT-ROM-1390-306
[11] Virgo Collaboration 2001 Measurement of the Virgo super-attenuator performance for seismic noise suppression *Rev. Sci. Instrum.* **72** 3643
[12] Fiori I 2008 *Noise from the Air Conditioning System* VIR-022A-2008
[13] *LineMonitor* web interface https://pub3.virgo.infn.it/itf/linemonitor
[14] Puppo P 2003 *A Finite Element Model of the Virgo Mirrors* VIR-NOT-ROM-1390-262